Analysis of Episodic Tremor and Slip in Cascadia Subduction Zone Using the Displacement and Strain Method

A Thesis Presented

by

Fang Qu

to

The Graduate School

in Partial Fulfillment of the

Requirements

for the Degree of

Master of Science

in

Geosciences

Stony Brook University

December 2014

Stony Brook University

The Graduate School

Fang Qu

We, the thesis committee for the above candidate for the

Master of Science degree, hereby recommend

acceptance of this thesis.

William Holt – Thesis Advisor

Professor, Department of Geosciences

Daniel Davis – Second Reader

Professor, Department of Geosciences

E. Troy Rasbury– Third Reader

Associate Professor, Department of Geosciences

This thesis is accepted by the Graduate School

Charles Taber

Dean of the Graduate School

Abstract of the Thesis

Analysis of Episodic Tremor and Slip in Cascadia Subduction Zone Using the Displacement and Strain Method

by

Fang Qu

Master of Science

in

Geosciences

Stony Brook University

2014

Recent studies have found a periodic phenomenon in some subduction zones called episodic tremor and slip (ETS). This kind of event can be detected by GPS stations and PBO stations. The ETS events can last 3-4 weeks and are generally correlated with non-volcanic tremor signals on seismometers. The Cascadia subduction zone has been divided into three ETS regions due to the variation of recurrence interval [Brudzinski and Allen, 2007], and most of the past studies that focused on the displacement field, have not analyzed the region for crustal strain patterns during the transient events. Stresses will be released during the ETS

events at the lower plate interface and then transfer onto the overlying plate above the locked megathrust zone. However, no past research has mapped the strain field within Cascadia during the ETS events, where such strains result from the imposed stresses. The purpose of this project is to create time-dependent strain maps of Cascadia during ETS events and characterize Cascadia slow slip in terms of mapped strain anomalies.

Contents

List of Figures

List of Tables

Introduction

1. What is Episodic Tremor and Slip (ETS)

In the Cascadia subduction zone, the denser oceanic plate is moving under the lighter continental plate. Although friction along the shallower plate interface fixes the two plates together, high temperatures at greater depth reduce the force of friction and let the two plates slip freely [Dragert et al., 2001]. Some of the GPS (Global Positioning System) sites have detected the transient surface deformation in terms of the slip events on the deeper (25- to 45-kilometer) part of the northern Cascadia subduction zone interface [Satake et al, 1996]. These slip events are accompanied by periods of tremor activity. These tremors can be detected in the subduction zone in the areas of the deep slip [Roger and Dragert, 2003] (Figure 1). This kind of phenomenon associated with tremor and slip is known as Episodic Tremor and Slip, short for ETS. During the ETS event, a large portion of accumulated stress will be released periodically in the transition zone between the locked and slipping region of the plate. These slow slips can last several weeks, which is different from the sudden slip of earthquakes. These ETS events can be detected with GPS and seismic stations. These events are characterized by reversed sense of motion (generally westward) during slow slip, lasting 3-4 weeks on average, and accompanied by increased aseismic (non-earthquake) tremor activity [Szeliga et al, 2008]. ETS is considered to relieve the stress in the transition region by transferring it to the earthquake zone and overriding crust, so it is important to understand ETS mechanisms and characteristics for the modeling of long-term crustal deformation and for modeling the mechanics of the ETS process.

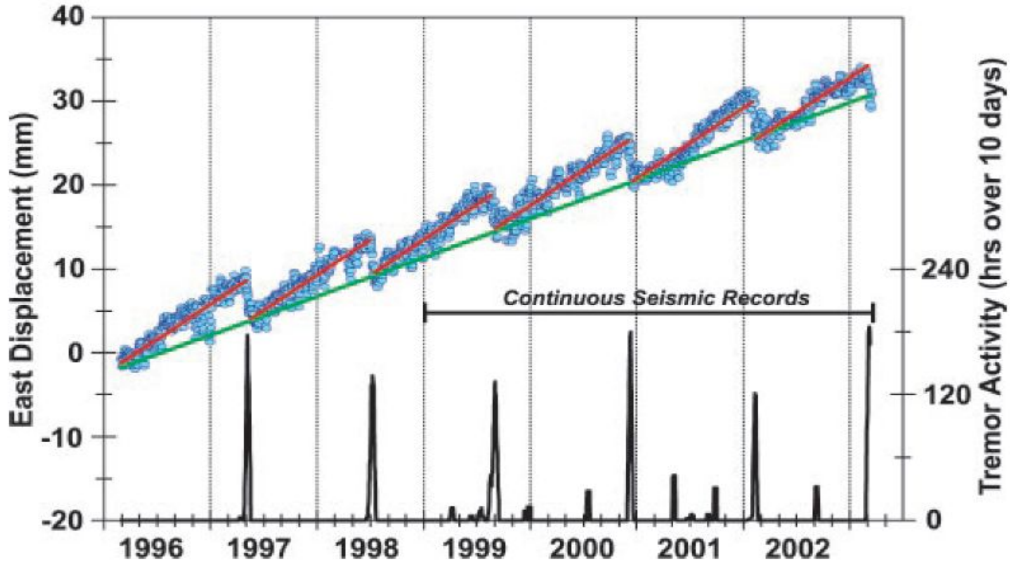

Figure 1: Comparison of slip and tremor activity detected in Cascadia subduction zone from Rogers and Dragert [Roger and Dragert, 2003].

2. Segmentation

Based on the observation of the Cascadia subduction zone, the features of ETS changed along strike, generating segmentations in terms of the variation of recurrence interval and relative timing of ETS events. Brudzinski and Allen [2007] found that there are three broad geographic zones of segmentation and each of them has its specific recurrence intervals of ETS behavior. (Figure 2) [Brudzinski and Allen, 2007]. This project will adopt strain field mapping techniques to examine Cascadia ETS in these three regions (Wrangellia Zone; Silezia Zone; Klamath Zone).

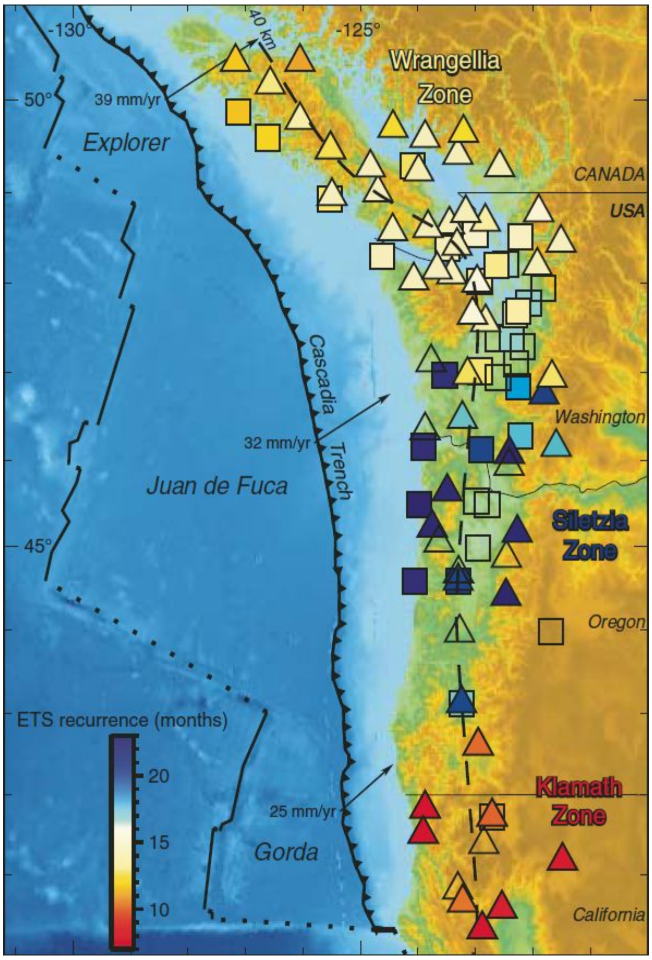

Figure 2: The segmentation classification in the Cascadia subduction zone from Brudzinski and Allen [2007]. It can be separated into three portions of Cascadia by the variation of recurrence interval: Wrangellia zone (14±2 months), Siletzia zone (19±3 months) and Klamath zone (10±2 months) [Brudzinski and Allen, 2007].

Most of the past studies focus on the major ETS events such as September 2005, January 2007, May 2008, August 2010, and August 2011, but recently, with the number of GPS stations increasing, many smaller ETS events have also been observed in Cascadia.

In past research on ETS, most workers were looking at the motions only and they use simple models of subduction to model these motions. No research to date has been conducted on the nature of the crustal strain patterns associated with ETS events. The details of the crustal strain associated with ETS events can provide important constraints on slip kinematics and dynamics. Previous research shows stress evolution is important to ETS manifestation and its effects. Previous ETS events have released an equivalent amount of strain from a moment magnitude of 6.7, which transfers stress into the seismogenic zone [Bartlow et al., 2011; Peng and Gomberg, 2010]. This stress transfer has significant implications for seismic hazard and the seismic cycle in general. Stress is inseparable from the entirety of ETS, and it can be elucidated by the quantification of strain within the region. The aim of this project is to illustrate and analyze ETS characteristics in accordance with strain associated crustal strain patterns. This analysis is based on the GPS data recorded over several ETS periods, showing strain and dilatation anomalies in Cascadia.

Methodology

1. Selection of GPS station data

To constrain the crustal deformation, GPS displacements are used. Therefore, the project begins with GPS station selection in Cascadia, on the basis of the large volume of data (Figure 3).

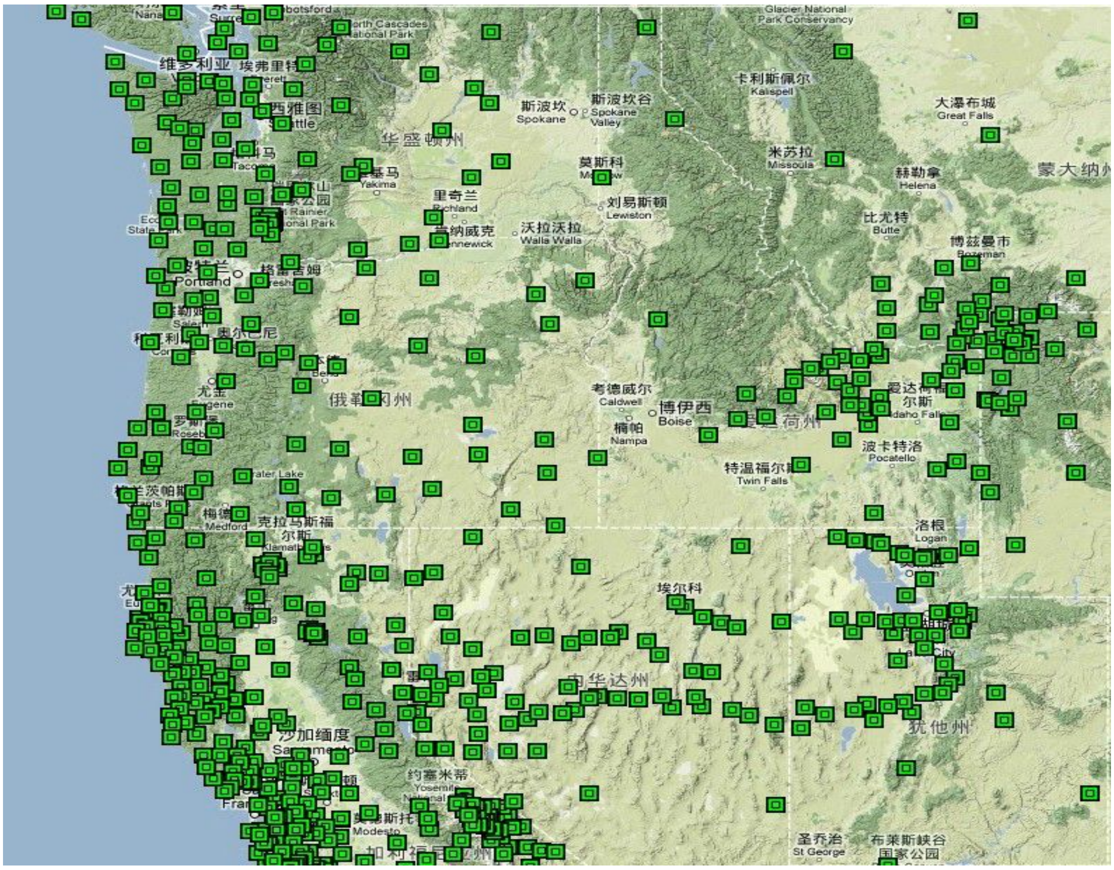

Figure 3: The distribution of GPS stations and PBO stations.

Prior to downloading the raw GPS data, the UNAVCO’s (a non-profit university-governed consortium that facilitates geoscience research and education using Geodesy.) data archive interface is applied to view the 228 GPS stations in Cascadia region (the Vancouver Island data is unavailable) of the Plate Boundary Observatory (PBO) network. Fifty-four GPS stations were removed to prevent the model from attempting to fit inaccurate data with following requirements:

(1) The raw GPS data should span from 2004.10 to 2012.50;
(2) Time series with excessive noise should be avoided;
(3) The stations with significant data gaps, wide fluctuations, or excessively unrealistic outliers should be avoided.

Nevertheless, the remaining stations distributed all over Cascadia did not leave an unbalanced data distribution in most areas.

2. Seasonal anomaly removal

By introducing the method of Holt and Shcherbenko [2013], the continuous GPS time series can be interpolated for gaining estimates of time-dependent displacements. This interpolation scheme removes estimates of seasonal signals and fits the residual time series with a moving average filter [Holt and Shcherbenko, 2013] (Figure 4).

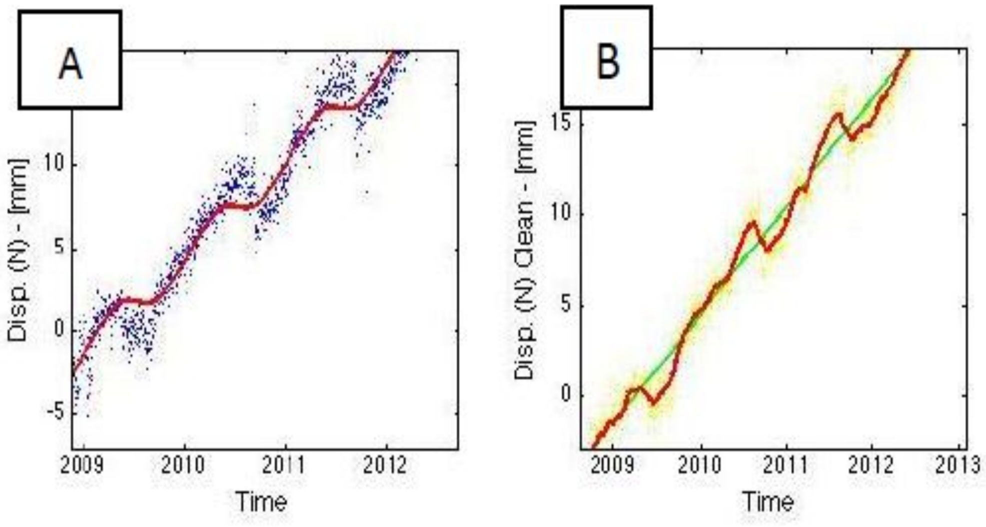

Figure 4: Time series (displacement vs. time) of station P418 (-123.4, 47.2) on the Olympic Peninsula. The blue dots in (A) are raw GPS data without seasonal removed. The red line is a low-order best-fit polynomial. In (B), the red line indicates the moving average and order polynomial (green line) are superimposed over GPS data with seasonal estimates removed.

3. Interpolation of displacements

The output provided by 174 stations displays displacements in time steps of 0.1yr, defining a regional time-dependent displacement field. The displacement field is then fit with bi-cubic spline functions to obtain a continuous estimate of strain and displacement over time. The following functional is minimized in the fitting procedure:

$$x = \sum_{cells\ ij,kl} \sum \left(\widehat{e_{ij}} - e_{ij}^{obs}\right)^T V_{ij,kl}^{-1} \left(\widehat{e_{kl}} - e_{kl}^{obs}\right) + \sum_{knots\ i,j} \sum \left(\widehat{u_i} - u_i^{obs}\right)^T V_{i,j}^{-1} \left(\widehat{u_j} - u_j^{obs}\right) \quad (1)$$

Where is the variance-covariance matrix of the strains, is the variance-covariance of the displacement, and are the model and observed strains, and and are the model and observed displacements [Holt and Shcherbenko, 2013].

A reference field obtained from time-averaged GPS (Figure 5; Figure 6) is subtracted from the time-dependent field to obtain a residual anomalous field [Holt and Shcherbenko, 2013].

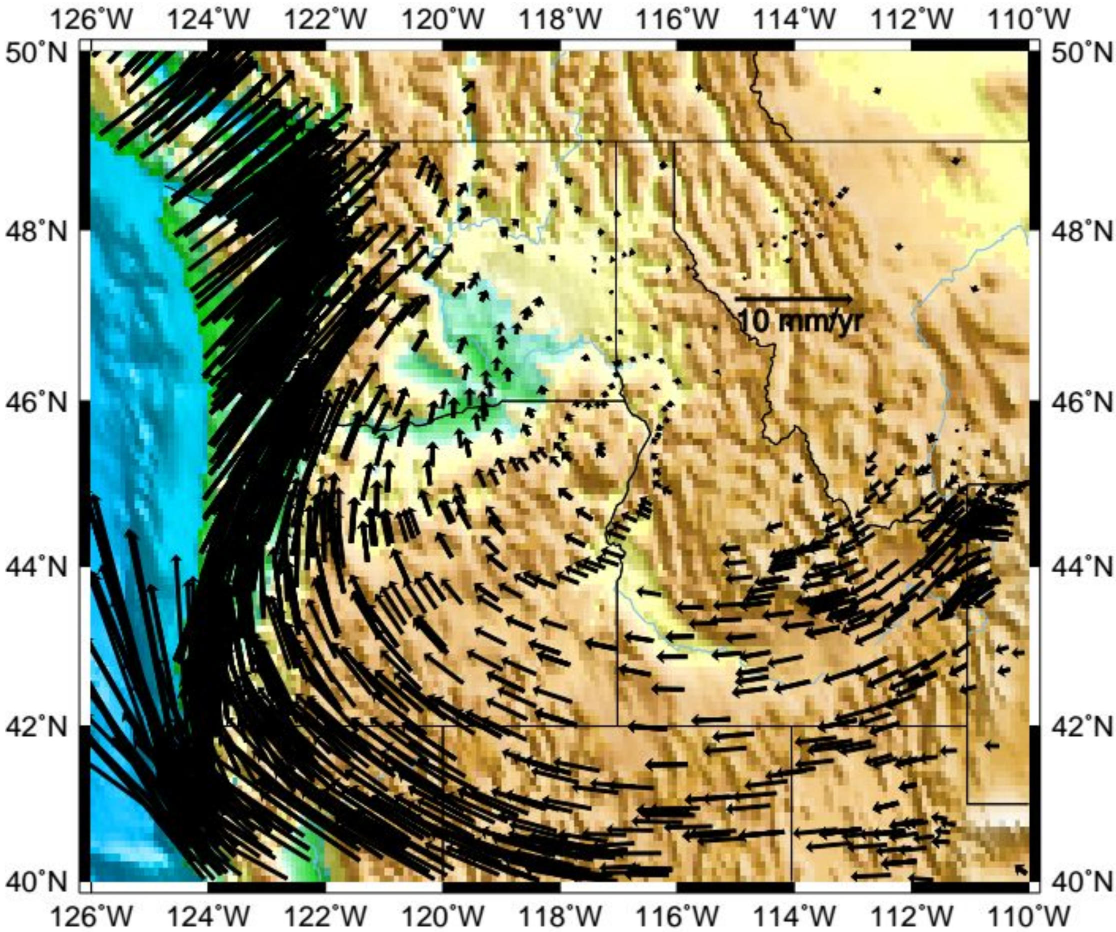

Figure 5: Velocity reference field, with motions relative to North America.

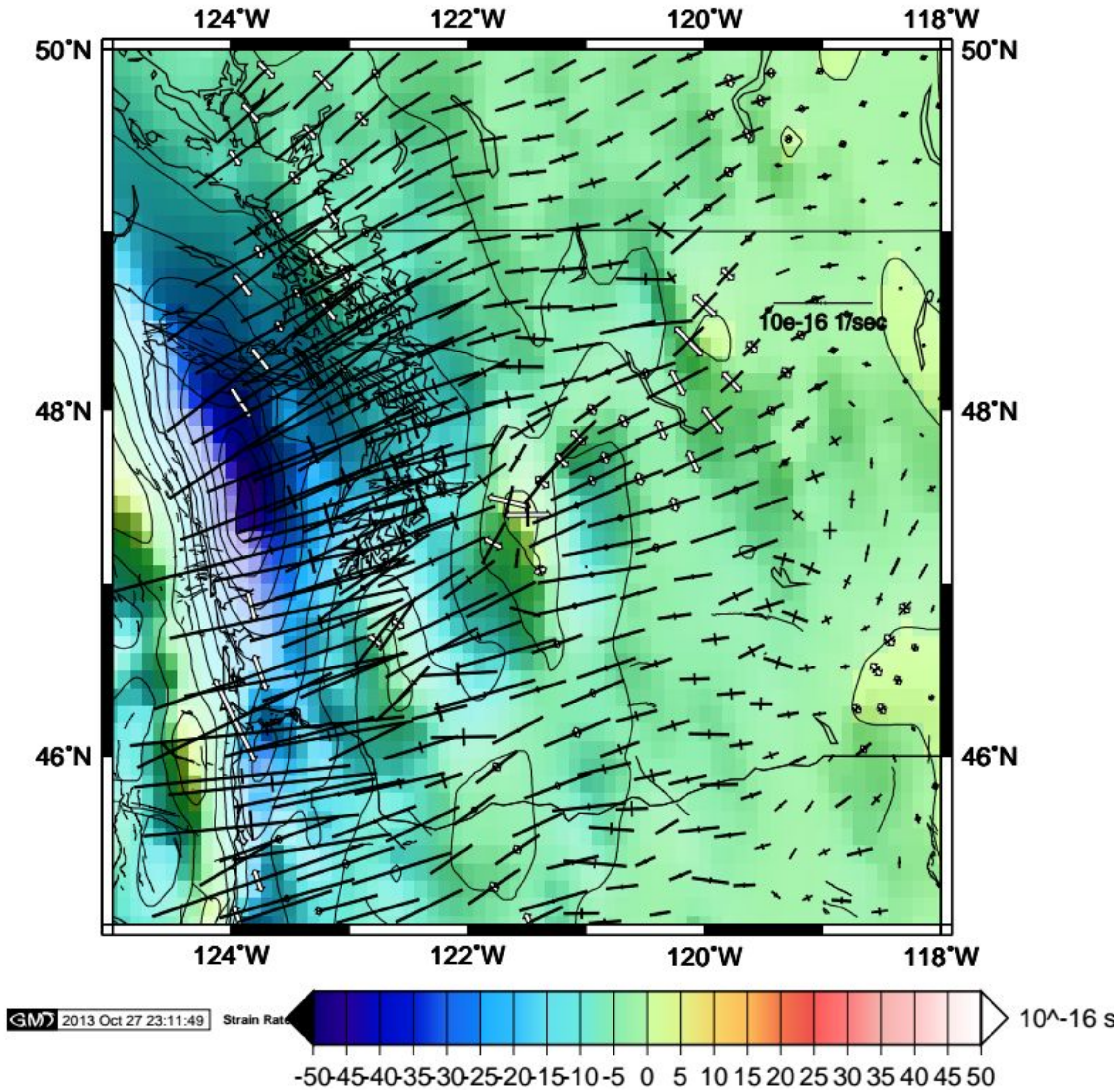

Figure 6: Strain reference field with contours of dilatation strain rate and principal axes of strain rate (white vectors are extension, bold vectors are compression).

Anomalous strain and displacement estimates (accumulated motions and strains over a 0.05 time period) are output in a moving time window of every 0.01 years. Movies of these anomalous strains and displacements were made and analyzed. Transient ETS events were identified based on coherence of displacement and anomalous strain signal, along with the duration of signal (Figure 7).

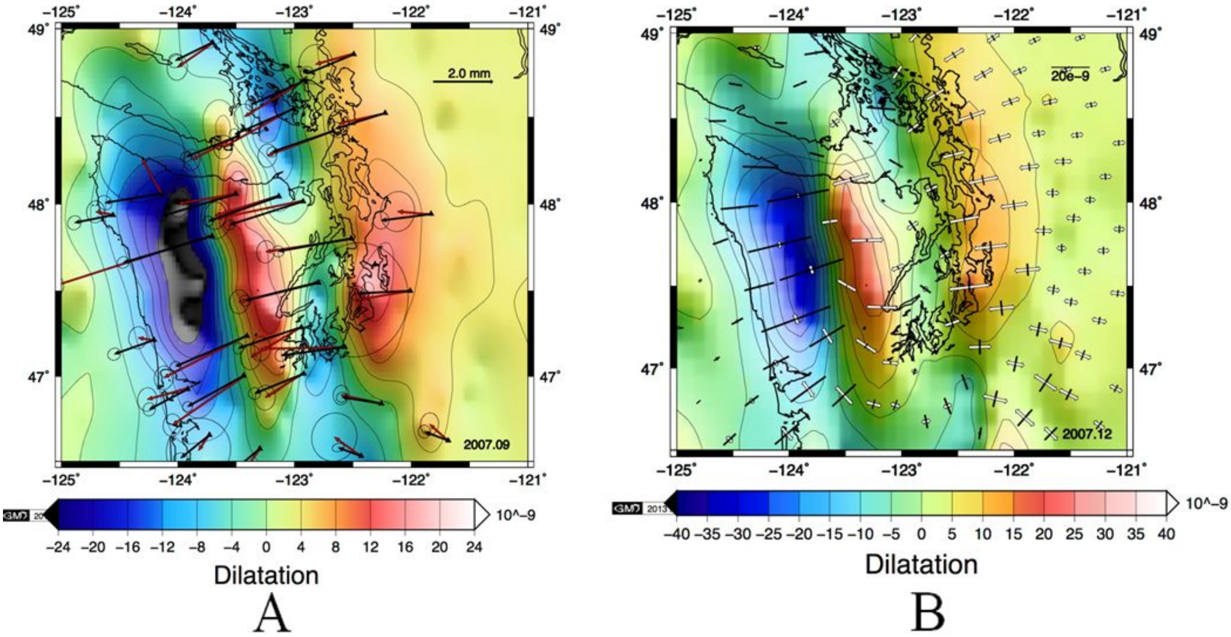

Figure 7: The residual strain field and displacement field maps for Northern Cascadia region during a 2007 ETS event. (A) Example snapshot of anomalous displacement field during an ETS event (red vector is residual observed displacement and bold is the model vector). (B) Example snapshot of anomalous strain field during the same ETS event. Contours are dilatation component of strain rate and principal axes of strain rate (white vectors are extension, bold vectors are compression).

Results

1. Northern Cascadia (Wrangellia zone)

In this region, there are seven ETS events that can be detected through examination of both the displacement field maps and the strain maps (2004.54_65; 2005.69_78; 2007.07_17; 2008.41_50; 2009.32_44; 2010.64_73; 2011.58_72) (Table 1).

Table 1

Event	Duration	Max Strain	Strain Direction	Time Evolution
N1	2004.54-2004.65	(southwest part) (northwest part)	W/E extension (normal slip) in the northeast part, NW/SE extension (mixed dip slip and strike slip) in the central part, NW/SE compression (thrust slip) in the southeast part, NE/SW compression (mixed dip slip and strike slip) in the northwest.	Vectors start pointing primarily southwest and then rotate clockwise 20 ° to 30 ° toward west.
N2	2005.69-2005.78	(southeast part) (southwest	W/E extension (normal slip) in the northeast part, W/E	Vectors start pointing primarily southwest and then rotate anticlockwise 20

		part)	compression (thrust slip) in the southwest part, NW/SE compression (strike slip) in the central part.	° to 30 ° toward south.
N3	2007.07-2007.17	(east part) (west part)	W/E extension (normal slip) in the eastern part, W/E compression (thrust slip) in the western part.	Vectors start pointing primarily southwest and then rotate clockwise 5 ° to 10 ° toward west.
N4	2008.41-2008.50	(northeast part) (west part)	W/E extension (normal slip) in the eastern part, W/E compression (thrust slip) in the western part.	Vectors start pointing primarily southwest and then rotate clockwise 20 ° to 30 °.
N5	2009.32-2009.44	(northeast part) (west part)	W/E extension (normal slip) in the eastern part, W/E compression (thrust slip) in the western part.	Vectors start pointing primarily southwest and then rotate clockwise 10 ° to 20 ° toward west.
N6	2010.60-2010.73	(northeast part) (west part)	W/E extension (normal slip) in the eastern part, W/E compression (thrust slip) in the western part.	Vectors start pointing primarily southwest and then rotate clockwise 5 ° to 10 °.
N7	2011.58-2011.72	(northeast part)	W/E extension (normal slip) in the eastern part, W/E	Vectors start pointing primarily southwest and then rotate

	(southwest part)	compression (thrust slip) in the western part.	anticlockwise 10 ° to 20 °.

As the Table 1 shows, the average duration of the ETS events in northern Cascadia is 10 epochs equivalence to roughly 1 month. The ETS events N1 and N2 have smaller magnitude in strain than the other ETS events in northern Cascadia. Most of the ETS events (N3; N4; N5; N6; N7) in northern Cascadia have a pure east-west W/E compression in the western area and pure east-west (W/E) extension to the east. Besides the pure east-west (W/E) compression and extension, more details of strain trend have been found during those ETS events, such as, NW/SE extension in the eastern part; NW/SE compression in the western part NE/SW compression in the northwest during the N1 event; NW/SE compression in the central part during the N2 event.

Furthermore, all the ETS events in northern Cascadia exists the similar dilatation distribution (although the N1 and N2 events are not very obvious because they lack sufficient data): two positive (extensional) dilatation lobes with a negative (compressional) lobe in between. The displacement vectors show an anticlockwise rotation pattern with shear strains present in the southwest-most dilatational lobe (Figure 8; Figure 9).

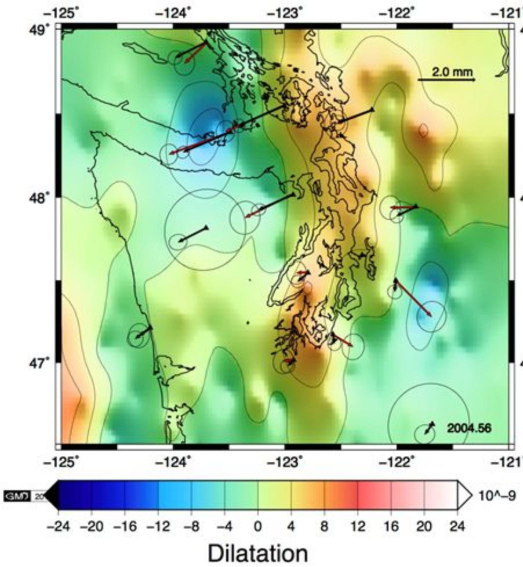
2.0 mm
2004.56
−125° −124° −123° −122° −121°
49° 48° 47°
10^−9
−24 −20 −16 −12 −8 −4 0 4 8 12 16 20 24
Dilatation

A

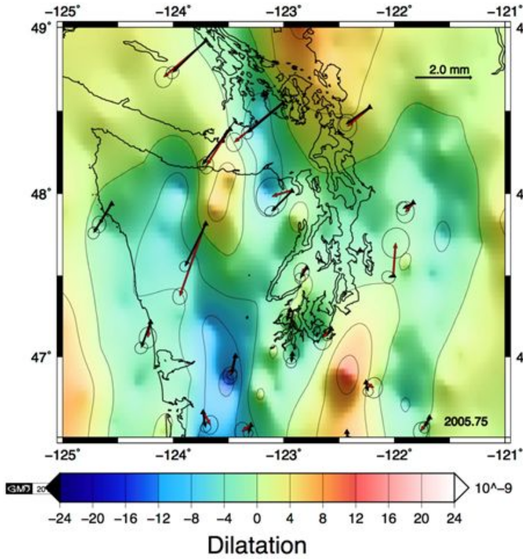
2.0 mm
2005.75
−125° −124° −123° −122° −121°
49° 48° 47°
10^−9
−24 −20 −16 −12 −8 −4 0 4 8 12 16 20 24
Dilatation

B

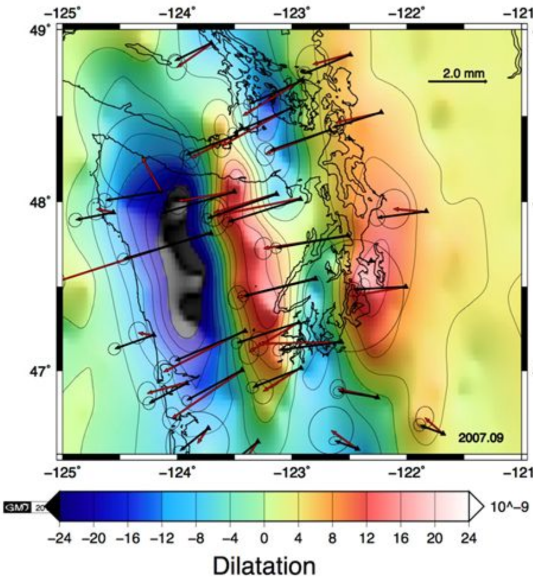
2.0 mm
2007.09
−125° −124° −123° −122° −121°
49° 48° 47°
10^−9
−24 −20 −16 −12 −8 −4 0 4 8 12 16 20 24
Dilatation

C

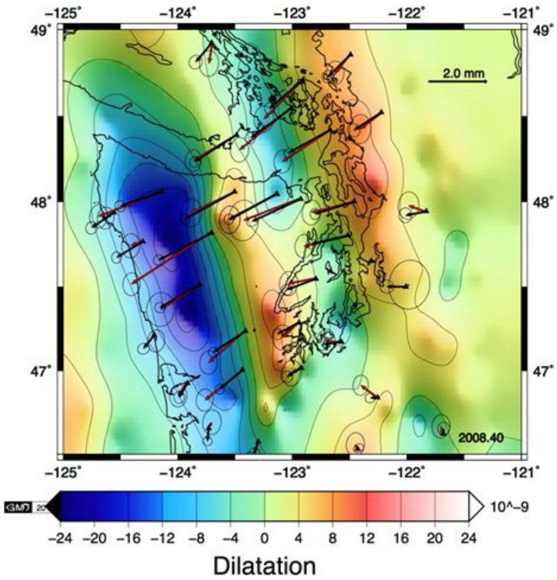
2.0 mm
2008.40
−125° −124° −123° −122° −121°
49° 48° 47°
10^−9
−24 −20 −16 −12 −8 −4 0 4 8 12 16 20 24
Dilatation

D

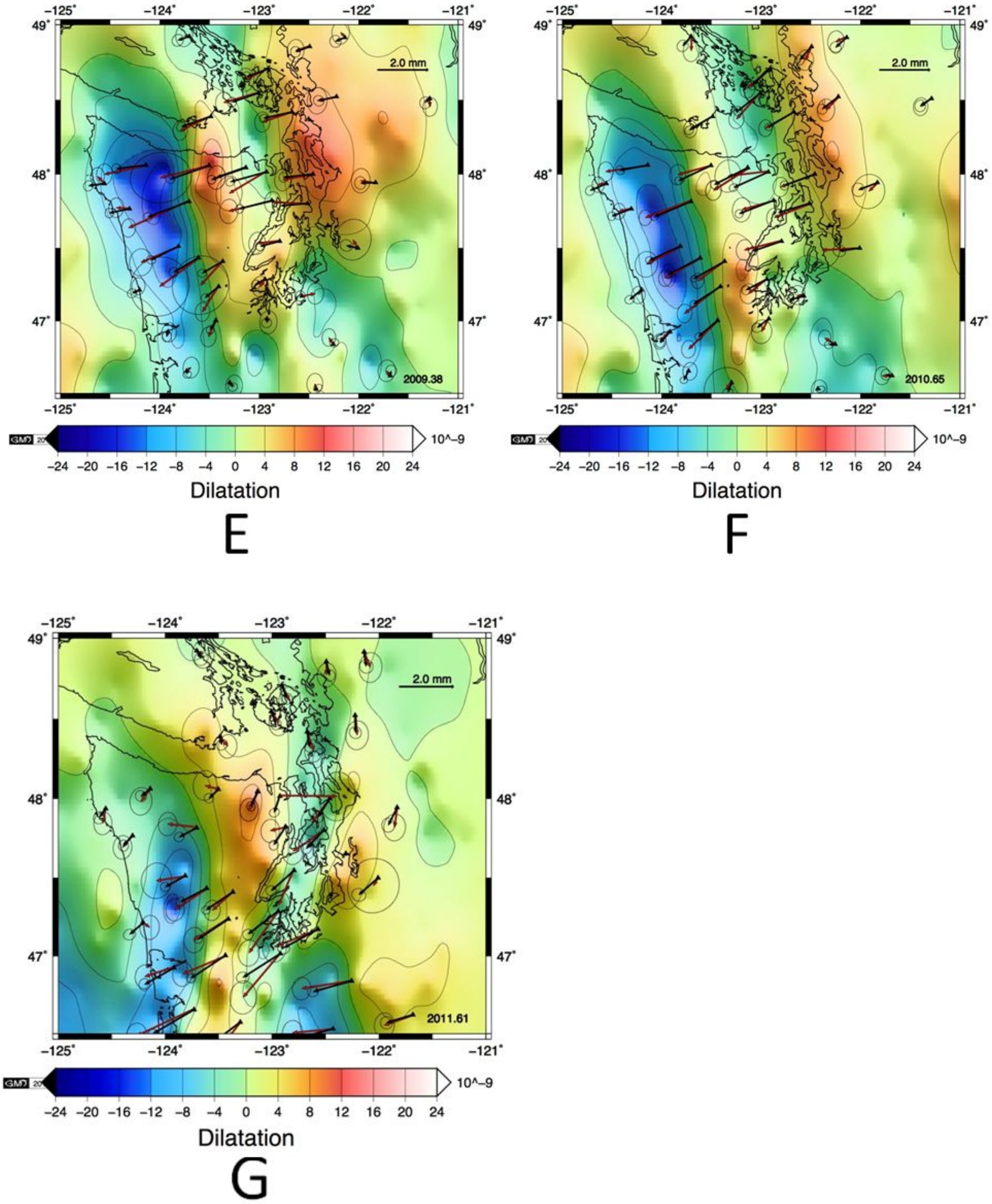

Figure 8: The anomalous displacement field map with contours of dilatation strain rate in northern Cascdia (triangles are GPS stations, red vector is residual observed displacement and bold is the model vector). (A) the anomalous displacement field map during N1 ETS event; (B) the anomalous displacement field map during N2 ETS event; (C) the anomalous displacement field map during N3 ETS event; (D) the anomalous displacement field map during N4 ETS event; (E) the anomalous displacement field map during N5 ETS event; (F) the anomalous displacement field map during N6 ETS event; (G) the anomalous displacement field map during N7 ETS event.

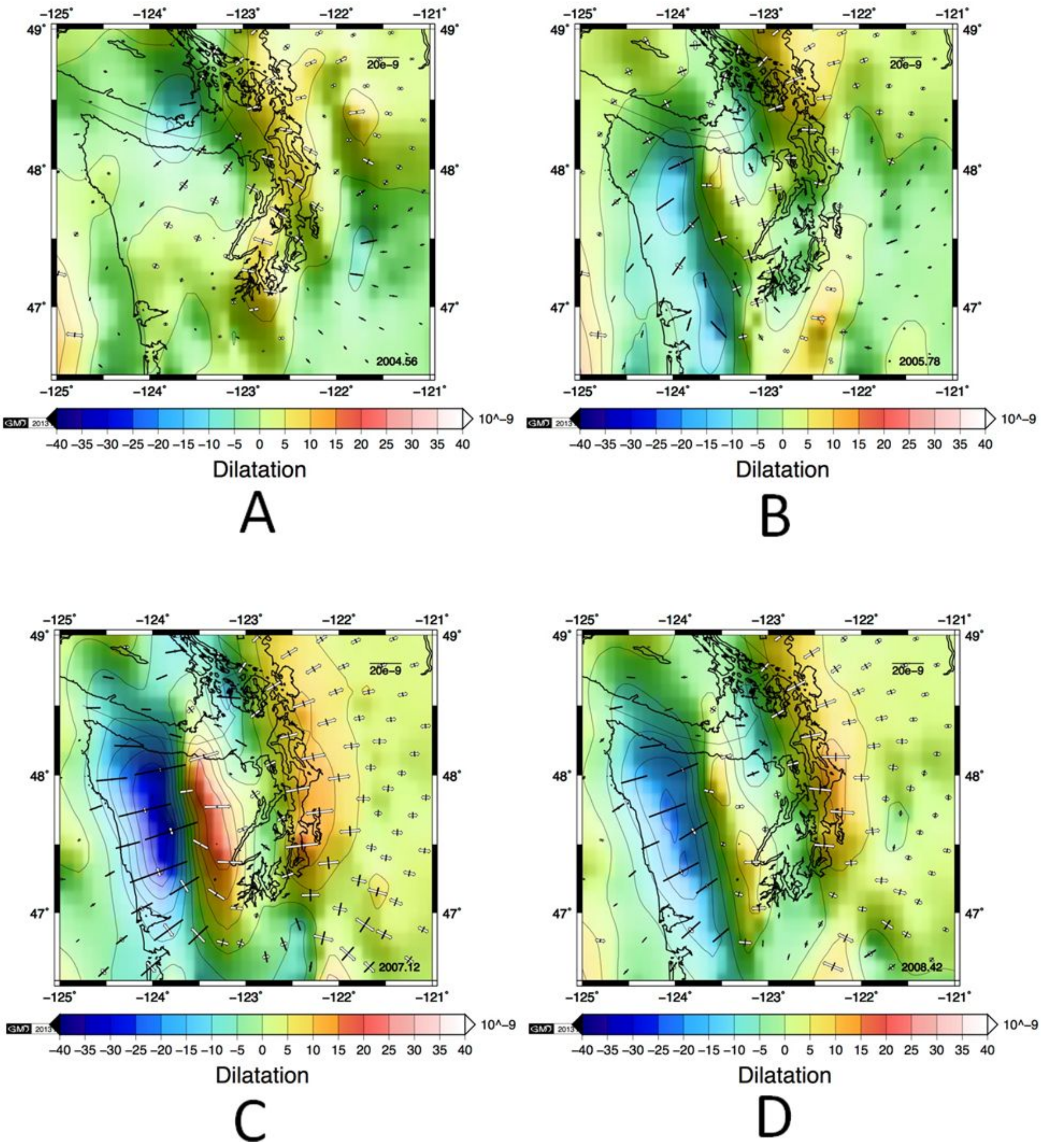
2004.56
20e-9
Dilatation
A
2005.78
20e-9
Dilatation
B
2007.12
20e-9
Dilatation
C
2008.42
20e-9
Dilatation
D

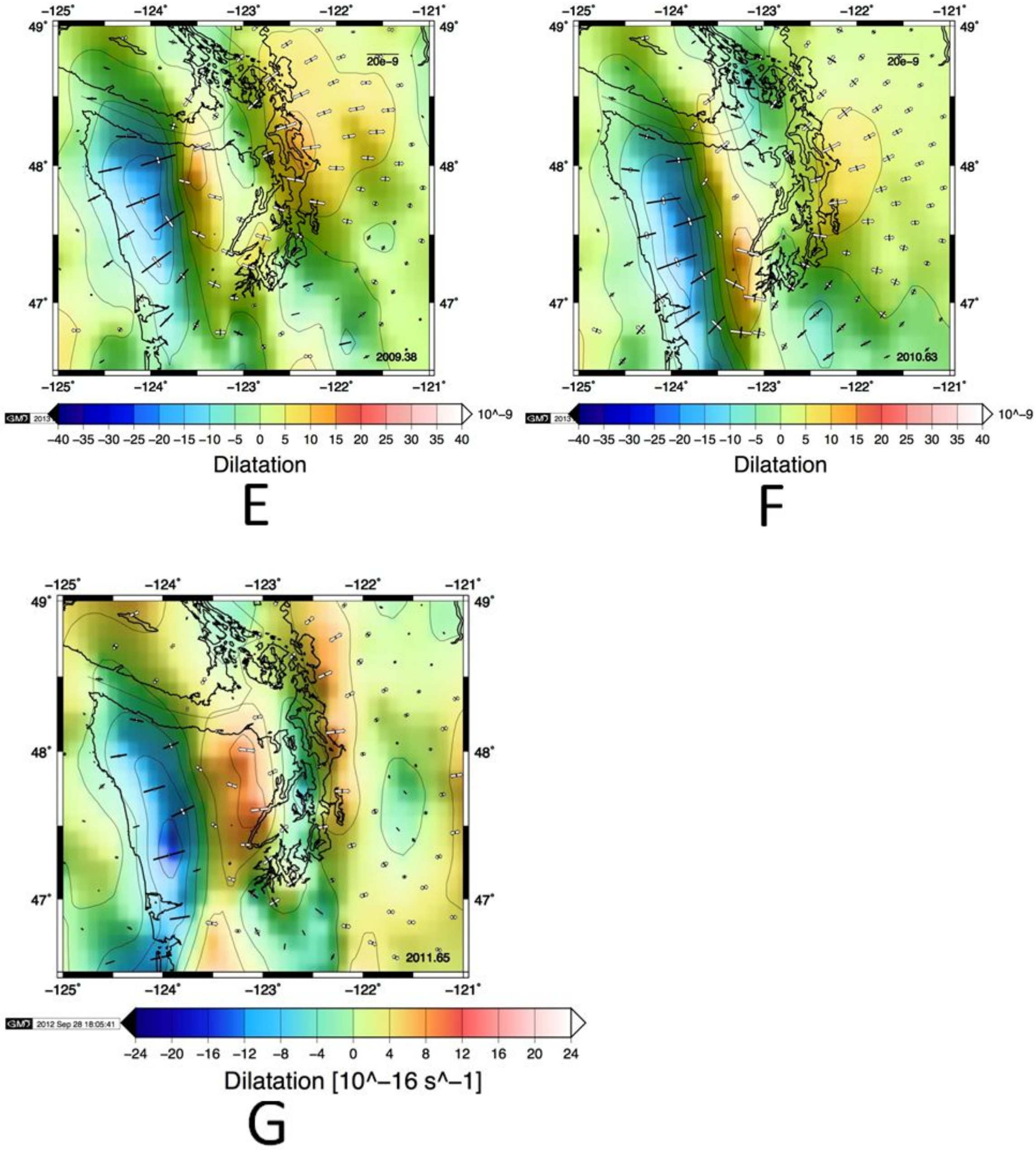

Figure 9: The anomalous strain field map with contours of dilatation strain rate and principle axes of strain rate (white axes are extension and black axes are compression) in the northern Cascadia. (A) the anomalous strain field map during N1 ETS event; (B) the anomalous strain field map during N2 ETS event; (C) the anomalous strain field map during N3 ETS event; (D) the anomalous strain field map during N4 ETS event; (E) the anomalous strain field map during N5 ETS event; (F) the anomalous strain field map during N6 ETS event; (G) the anomalous strain field map during N7 ETS event.

2. Central Cascadia (Siletzia zone)

Central Cascadia is less straightforward than the northern Cascadia zone in regard to strain and displacement anomalies. In terms of the mapping of displacement, central Cascadia ETS events show migrations of displacement over a large number of directions and magnitudes. In addition, vectors in surrounding groups are not as consistent as are displayed in the northern Cascadia. There are five ETS events that can be detected both in the displacement field maps and strain field maps (2007.36_55; 2008.35_45.; 2009.64_72; 2010.17_26; 2011.49_58) (Table 2).

Table 2

Event	Duration	Max Strain	Strain Direction	Time Evolution
C1	2007.36-2007.55	$+6\times10^{-9}$ (west part) -3×10^{-9} (east part)	W/E and N/S extension (normal slip) in eastern part, W/E compression (thrust slip) in the western part.	Vectors start pointing primarily southwest and rotate clockwise 20 ° to 30 ° toward northwest, then rotate anticlockwise 50 ° to 60 ° toward southwest
C2	2008.35-2008.45	$+12\times10^{-9}$ (east part) -3×10^{-9} (west part)	W/E extension (normal slip) in eastern part, W/E compression (thrust slip) in the western part.	Vectors start pointing primarily southwest and then rotate clockwise 5 ° to 10 ° toward west.
C3	2009.64-2009.72	$+12\times10^{-9}$ (northwest part)	W/E extension (normal slip) and NW/SE	Vectors start pointing primarily southwest and

		-16×10^{-9} (northeast part)	extension (mixed dip slip and strike slip) in the eastern part, W/E compression (thrust slip) and NE/SW compression (mixed dip slip and strike slip) in the western part.	then rotate clockwise 10 ° to 20 ° toward west.
C4	2010.17-2010.26	$+12 \times 10^{-9}$ (northeast part) -9×10^{-9} (northwest part)	W/E extension (normal slip) in the eastern part, W/E compression (thrust slip) in the western part.	No displacement rotation.
C5	2011.49-2011.58	$+16 \times 10^{-9}$ (east part) -16×10^{-9} (west part)	W/E extension (normal slip) and N/S extension (mixed dip slip and strike slip) in the eastern part, W/E compression (mixed dip slip and strike slip) and N/S compression (thrust slip) in the western part.	Vectors start pointing primarily southwest and then rotate clockwise 5 ° to 10 °.

As shown in Table 2, the ETS events in central Cascadia have an average duration of 9 epochs, equivalent to roughly 4 weeks, which is less than the average duration in northern Cascadia. The average magnitude of the displacements and strains are much smaller than that of the northern Cascadia ETS events as well. Overall, the details of strain trend in this region are not as obvious or as consistent with that of the northern Cascadia ETS events. The C1, C3, C5 events have a similar distribution of strain patterns: they exhibit extension in the eastern part and compression in the western part. For the dilatation, two positive (extensional) dilatation lobes with a negative (compressional) lobe in between can be observed in both of the displacement field maps and strain field maps. The displacement vectors show a counterclockwise rotation pattern with significant shear strains present in the western-most dilatational lobe.

For the C2 event, there exists a similar dilatation distribution as C1, C3 and C5 events, but there is no rotation (and associated shear strain) of the displacement vector field like there is for C1, C3 and C5. The dilatation distribution of the C4 event is different from other ETS events in the central Cascadia, and there is no shear strain and displacement vector rotation can be found as well (Figure 10; Figure 11).

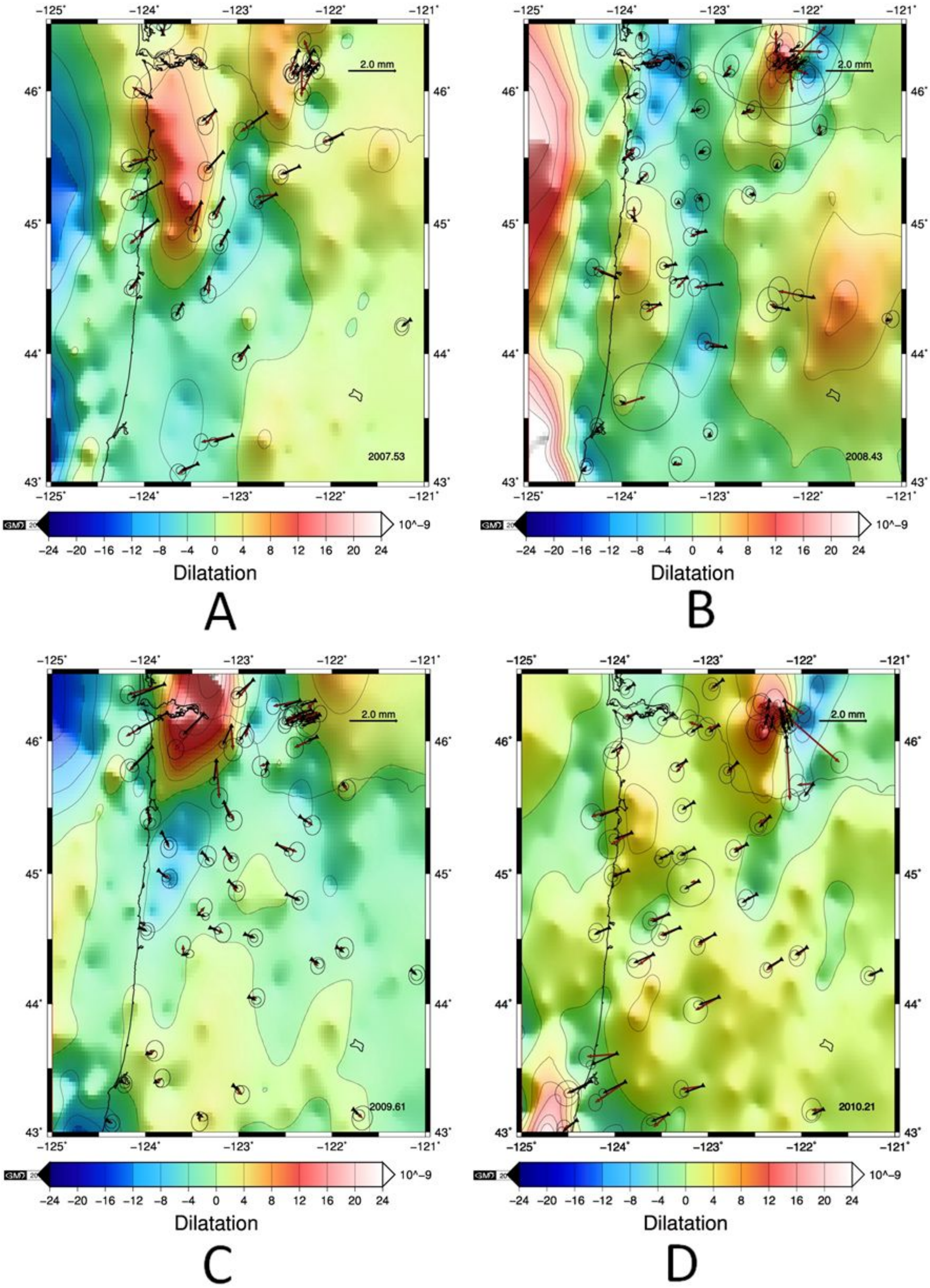

−125˚
−124˚
−123˚
−122˚
−121˚
46˚
45˚
44˚
43˚
2.0 mm
2007.53
2008.43
2009.61
2010.21
−24 −20 −16 −12 −8 −4 0 4 8 12 16 20 24
10^−9
Dilatation
A
B
C
D

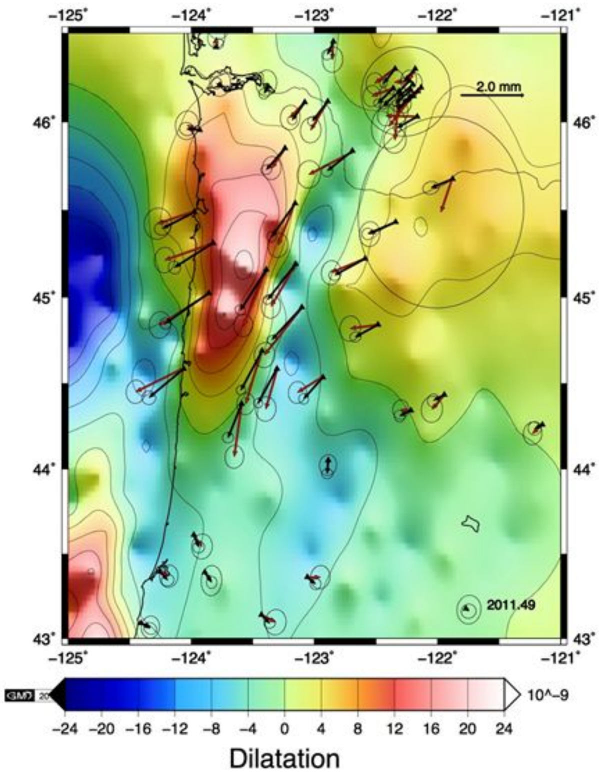

E

Figure 10: The anomalous displacement field map with contours of dilatation strain rate in central Cascdia (triangles are GPS stations, red vector is residual observed displacement and bold is the model vector). (A) the anomalous displacement field map during C1 ETS event; (B) the anomalous displacement field map during C2 ETS event; (C) the anomalous displacement field map during C3 ETS event; (D) the anomalous displacement field map during C4 ETS event; (E) the anomalous displacement field map during C5 ETS event.

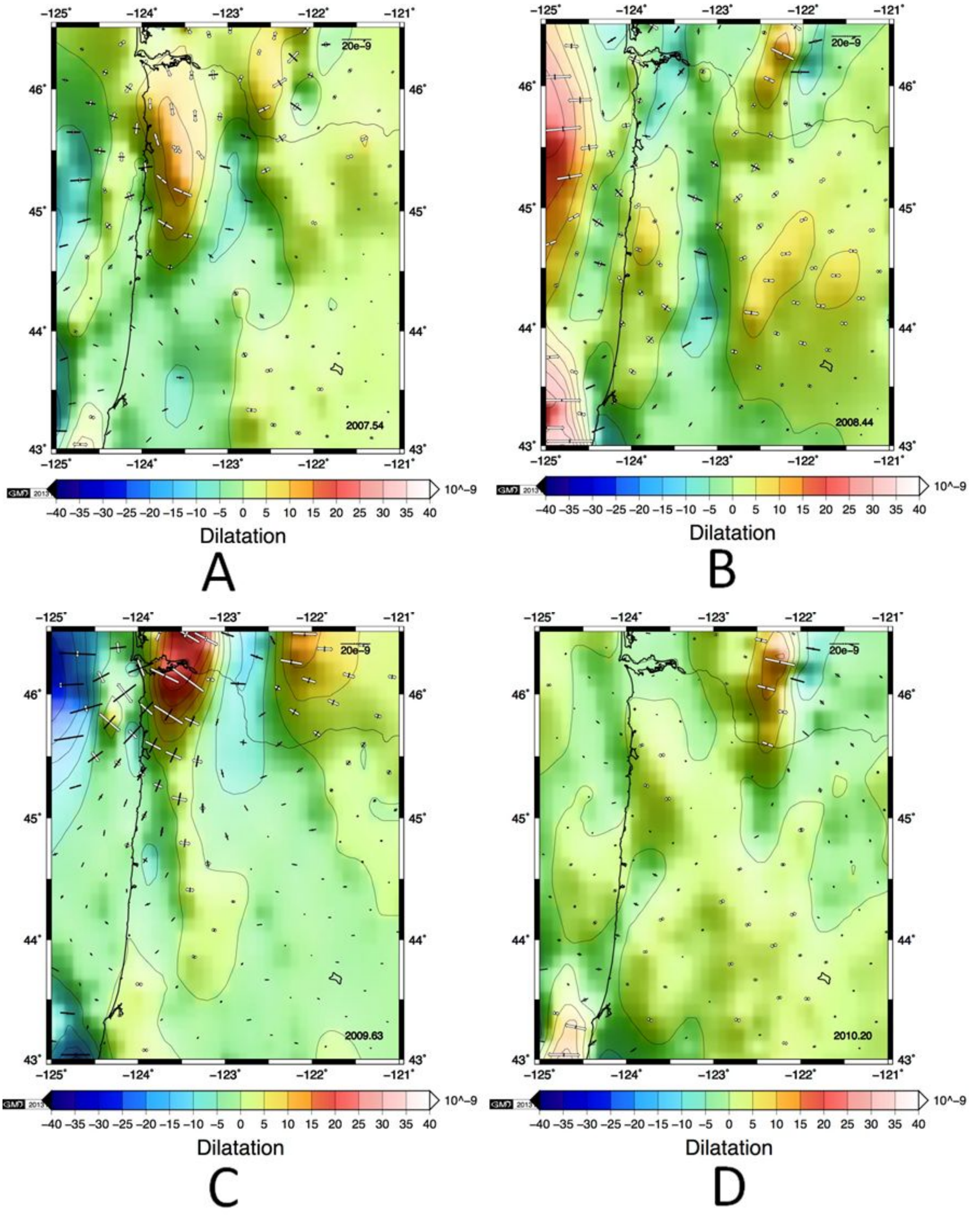
2007.54
20e-9
Dilatation
10^-9
A
2008.44
20e-9
Dilatation
10^-9
B
2009.63
20e-9
Dilatation
10^-9
C
2010.20
20e-9
Dilatation
10^-9
D

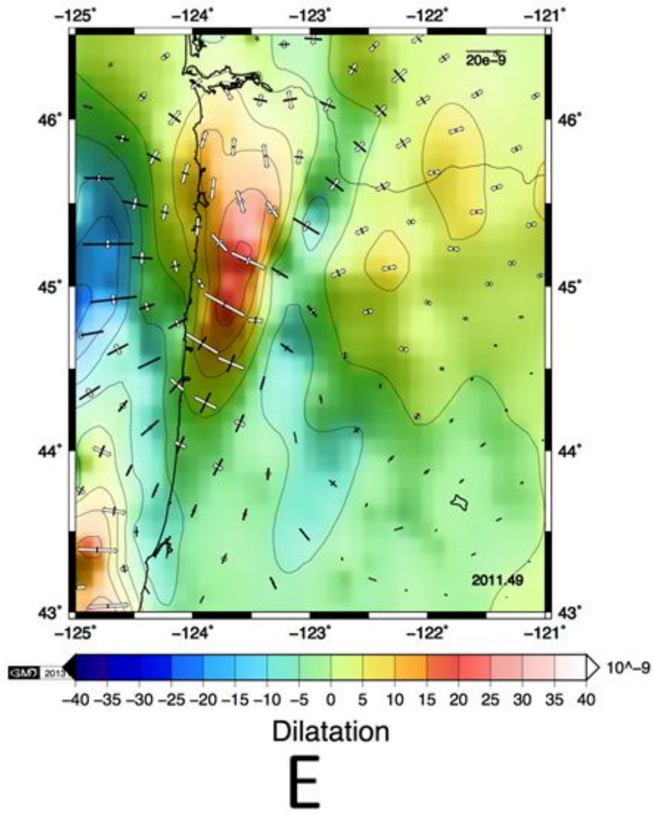

Figure 11: The anomalous strain field map with contours of dilatation strain rate and principle axes of strain rate (white axes are extension and black axes are compression) in the central Cascadia. (A) the anomalous strain field map during C1 ETS event; (B) the anomalous strain field map during C2 ETS event; (C) the anomalous strain field map during C3 ETS event; (D) the anomalous strain field map during C4 ETS event; (E) the anomalous strain field map during C5 ETS event.

3. Southern Cascadia (Klamath zone)

The ETS events in southern Cascadia have not only the largest magnitude of strain trend but also the largest duration (11 epochs equivalent to roughly 1 and a half months) among the three regions. There are seven ETS events that can be detected through both the displacement field maps and strain field maps, which occur with a higher frequency than that of central ETS events. (2004.84_92; 2005.45_54; 2006.73_94; 2007.69_79; 2008_9.95_05; 2010.00_11; 2011.12_22) (Table 3).

Table 3

Event	Duration	Max Strain	Strain Direction	Time Evolution
S1	2004.84-2004.92	(southwest part) (southeast part)	W/E extension (normal slip) and NW/SE extension (mixed dip slip and strike slip) in the western part, W/E compression (thrust slip) in the eastern part.	Vectors start pointing primarily southeast and then rotate clockwise 5° to 10° toward east.
S2	2005.45-2005.54	(southwest part) (southeast part)	W/E extension (normal slip) and N/S extension (mixed dip slip and strike slip) in the western part, W/E compression (thrust slip) in the eastern part.	Vectors start pointing primarily southeast and then rotate anticlockwise 5° to 10° toward south.
S3	2006.73-2006.94	(southwest part) (southeast part)	W/E extension (mixed dip slip and strike slip) in the southeast, W/E compression (thrust slip) in the western part.	Vectors start pointing primarily southwest and then rotate anticlockwise 260° to 270° toward northwest.
S4	2007.69-2007.79	(southwest	W/E extension (normal slip)	Vectors start pointing primarily

		part) (southeast part)	in the eastern part, W/E compression (thrust slip) and NW/SE compression (mixed dip slip and strike slip) in the western part.	southwest and then rotate anticlockwise 140 ° to 150 ° toward east.
S5	2008.95-2009.05	(southwest part) (southeast part)	W/E extension (normal slip) in the southeast part, W/E compression (thrust slip) in the northwest part.	No displacement rotation.
S6	2010.00-2010.11	(southwest part) (southeast part)	W/E extension (mixed dip slip and strike slip) in the eastern part, NW/SE compression (thrust slip) and N/S compression (mixed dip slip and strike slip) in the western part.	No displacement rotation.
S7	2011.12-2011.22	(southwest part) (southeast part)	W/E extension (normal slip) in the southeast part, W/E compression in the western part.	Vectors start pointing primarily west and then rotate clockwise 5 ° to 10 ° toward northwest.

The S3, S5, S7 events have a similar strain pattern (extension in the eastern part and compression in the western part) which is much different from the S1, S2, S4 and S6 events. Furthermore, this region has also shown a complex distribution of strain trends, the S1, S2, S4 and S6 event are not consistent with back-slip on the meagathrust (it should be compression in western part and extension in eastern part) and need to be investigated further.

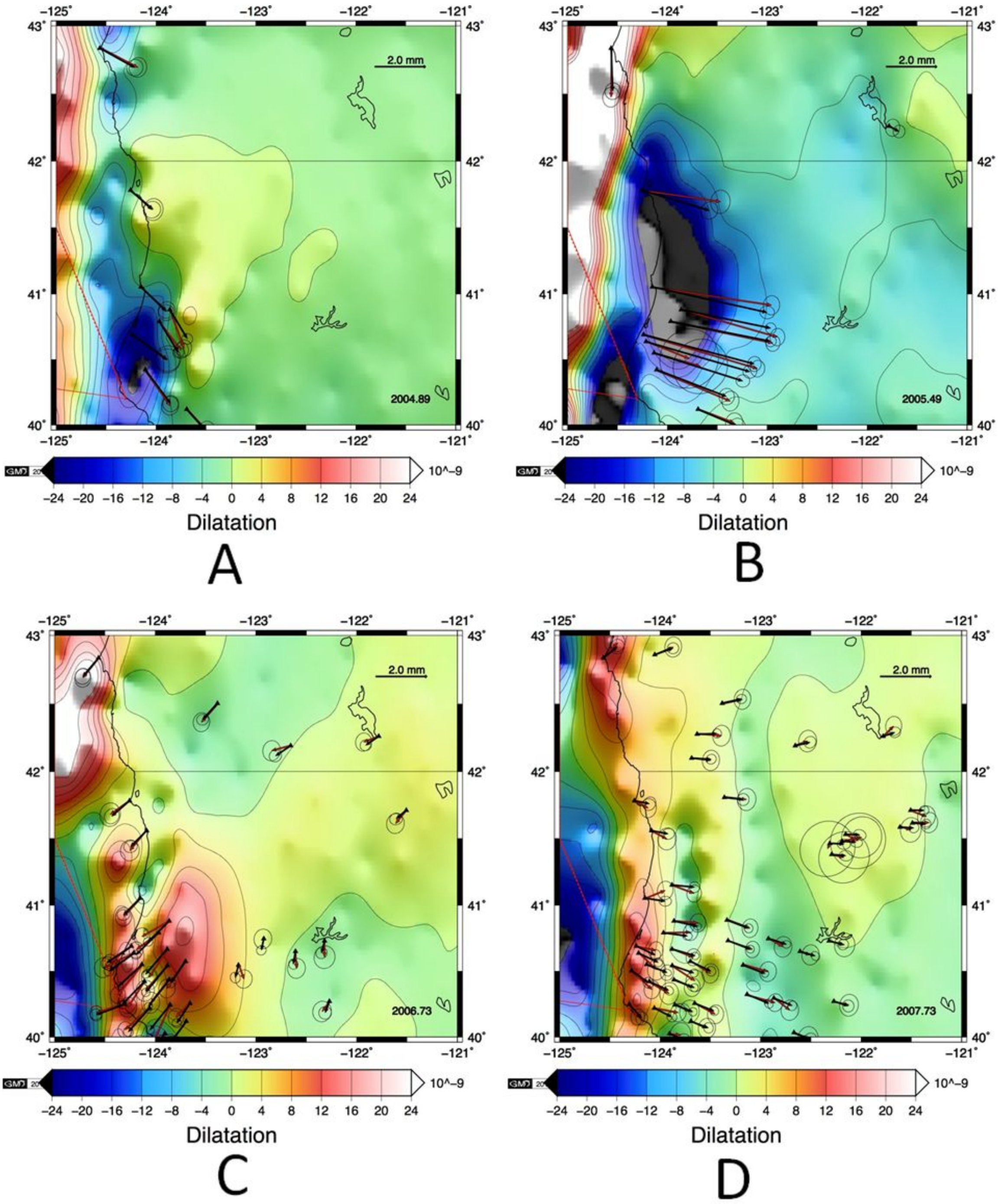

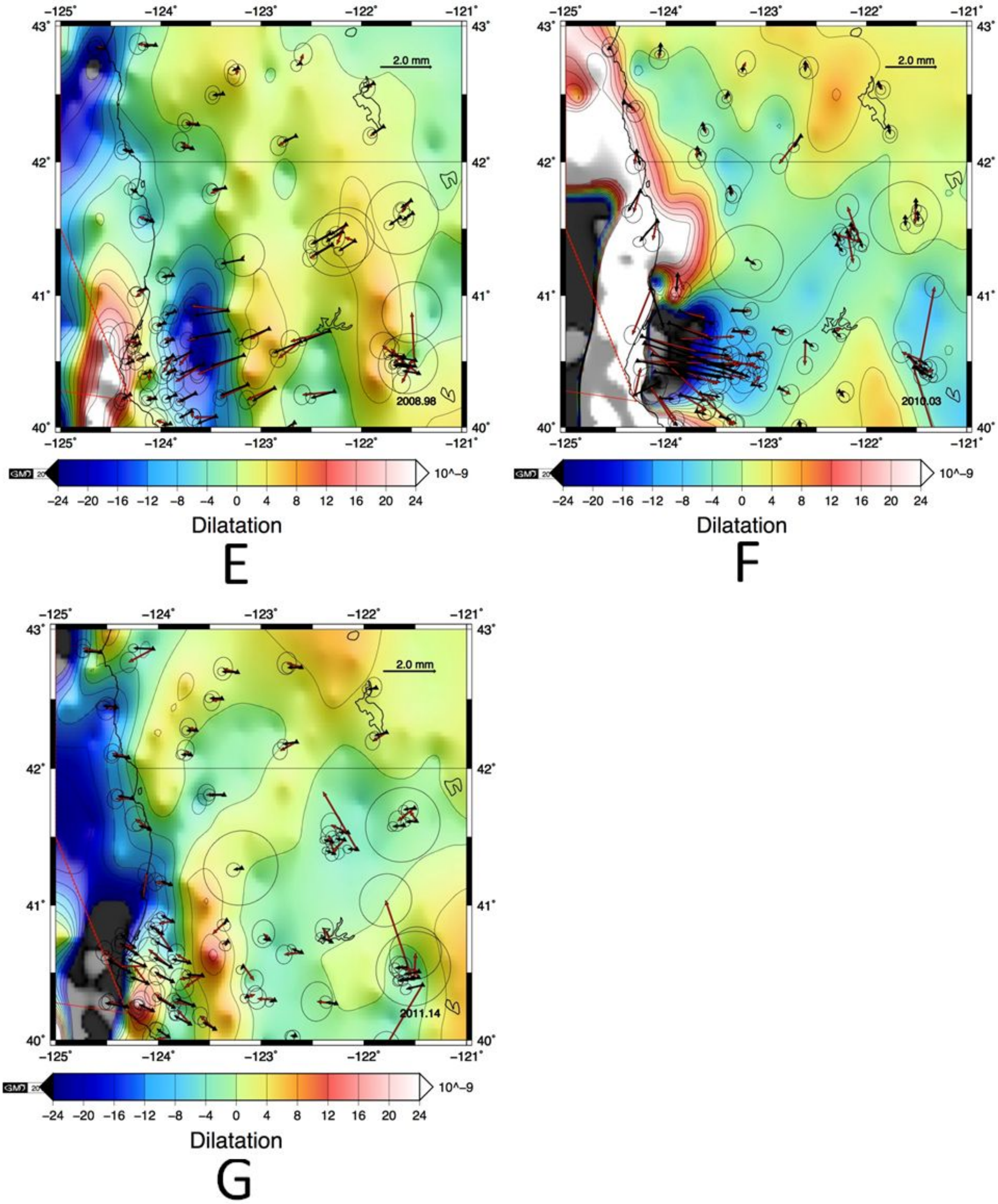

Figure 12: The anomalous displacement field map with contours of dilatation strain rate in southern Cascdia (triangles are GPS stations, red vector is residual observed displacement and bold is the model vector). (A) the anomalous displacement field map during S1 ETS event; (B) the anomalous displacement field map during S2 ETS event; (C) the anomalous displacement field map during S3 ETS event; (D) the anomalous displacement field map during S4 ETS event; (E) the anomalous displacement field map during S5 ETS event; (F) the anomalous displacement field map during S6 ETS event; (G) the anomalous displacement field map during S7 ETS event.

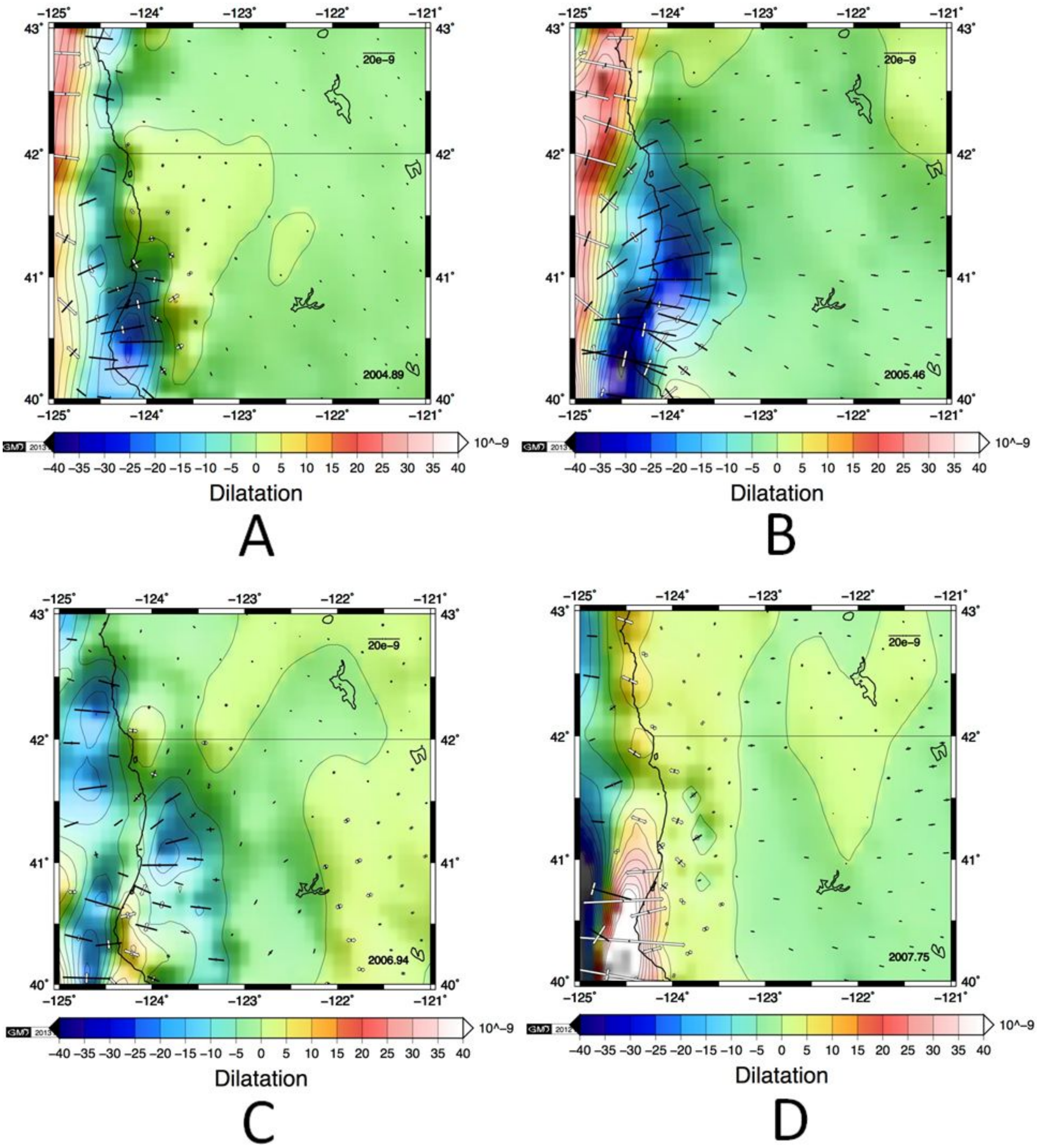
20e-9
2004.89
Dilatation
A
2005.46
Dilatation
B
2006.94
Dilatation
C
2007.75
Dilatation
D
10^-9

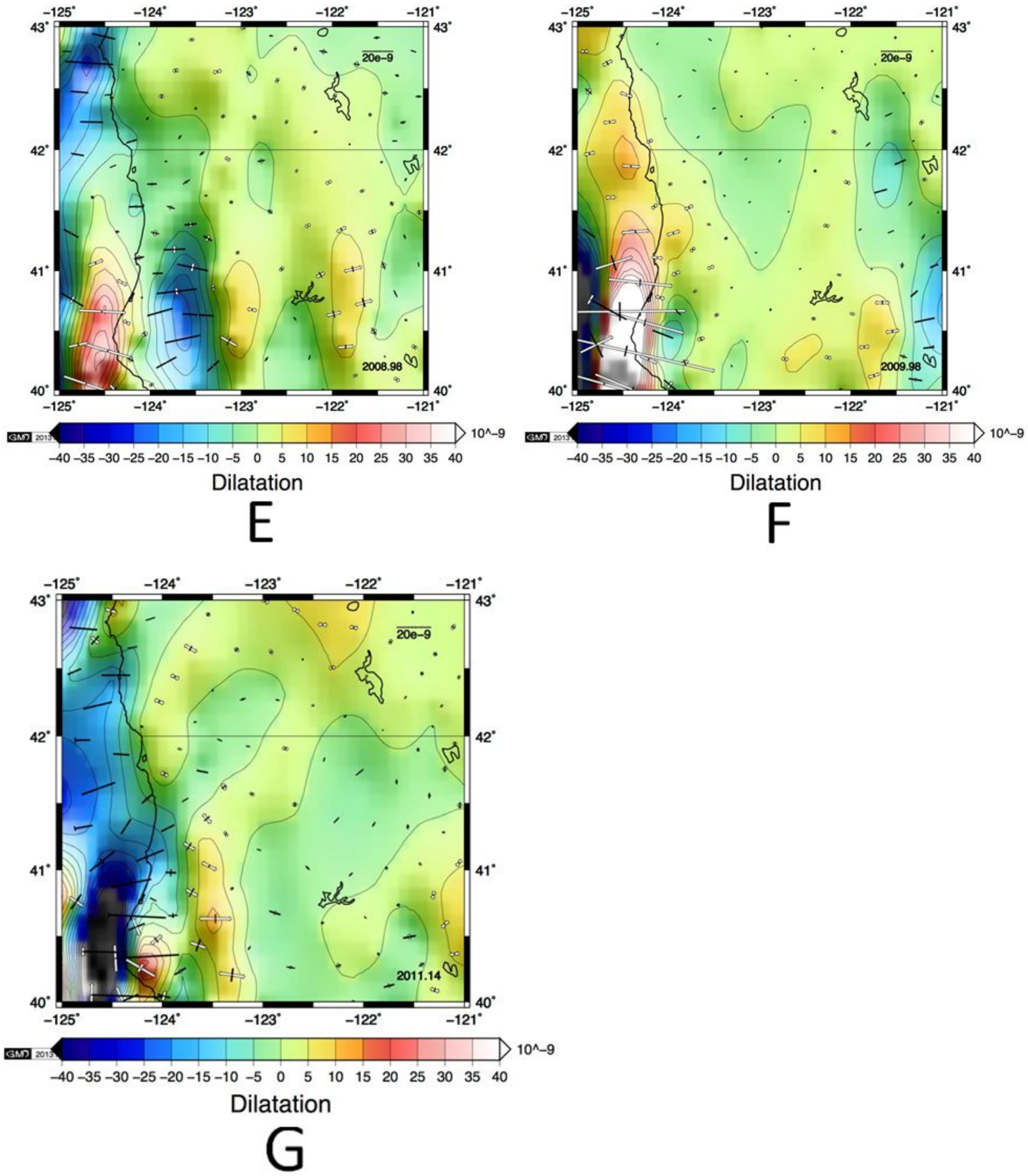

Figure 13: The anomalous strain field map with contours of dilatation strain rate and principle axes of strain rate (white axes are extension and black axes are compression) in the southern Cascadia. (A) the anomalous strain field map during S1 ETS event; (B) the anomalous strain field map during S2 ETS event; (C) the anomalous strain field map during S3 ETS event; (D) the anomalous strain field map during S4 ETS event; (E) the anomalous strain field map during S5 ETS event; (F) the anomalous strain field map during S6 ETS event; (G) the anomalous strain field map during S7 ETS event.

Conclusion and discussion

Although there are different characteristics within and between ETS events, the additional information embedded in the strain field holds promise for providing important new constraints. Strain field analysis can provide additional insight into the intrinsic properties of each ETS event, and can provide vital constraints on directions of stress transfer within different regions of the overlying plate. Analysis of the continuous GPS time series in the way that is done here shows the temporal and spatial correlations of the displacement and strains during ETS events.

In this research, the duration of ETS events in northern Cascadia is 10 epochs (roughly thirty-six days) and that of central Cascadia is 9 epochs (roughly thirty-two days), which is consistent with the previous findings [Aguiar et al., 2009]. However, the duration of southern Cascadia (roughly forty days) is slightly longer than those in northern Cascadia and central Cascadia. The ETS events in northern Cascadia repeated on an average of 115 epochs, equivalent to 14 months, in agreement with Brudzinski and Allen [2007]. Nevertheless, the recurrence interval in central and southern Cascadia is different from Brudzinski's findings. The reason is that Brudzinski's method only applies to the major ETS events, but I found several medium and small events, which the strain analysis has revealed.

Furthermore, most of the ETS events show the consistency with a back-slip in the strain field maps (compression in the western part and extension in the eastern part). Some of them, such as C2, C4, S1, S2, S4, S6 events, show complexity and are not easily linked with simple back-slip on the megathrust. The cause of these unusual strain anomalies could be another fault involved other than the megathrust. Such a fault may lie within the overlying crustal wedge. However, these complicated strain anomalies, how they relate to potential deformation of the subduction thrust, or possibly other fault features, need to be investigated further.

References

A. C. Aguiar et al, Moment release rate of Cascadia tremor constrained by GPS, Journal of Geophysical Research, 2009, **114**, B00A05.

A. G. Wech et al, A continuum of stress, strength, and slip in the Cascadia transition zone, Nature Geoscience, 2011, **4**, 1-5.

A. G. Wech et al, Seismic and geodetic constraints on Cascadia slow slip, Journal of Geophysical Research, 2009, **144**, B10316.

B. F. Atwater et al, Recurrence intervals for great earthquakes of the past 3,500 years at northeastern Willapa Bay, WashingtonL U.S Geological Survey Professional Paper, 1997, **1576**, 108.

B. R. Brudzinski et al, Segmentation in episodic tremor and slip all along Cascadia, Geology, 2007, **35** (10), 907-910.

B. Shen-Tu et al, The contemporary kinematics of the Western United States estimated from Quaternary rates of slip and space geodetic data, Journal of Geophysical Research, 1999, **104**, 28927-28955.

D. Shelly et al, Triggered creep as possible mechanism for delayed dynamic triggering of tremor and earthquakes, Nature Geoscience, 2011, **4**, 383, 388.

G. Rogers et al, Episodic tremor and slip on the Cascadia subduction zone, Science, 2003, **300** (5627).

G. Rogers et al, Episodic tremor and slip on the Cascadia subduction zone: the Chatter of Silent Slip, Science, 2003, **300** (5627).

H. Dragert et al, A silent slip event on the deeper Cascadia subdction interface, Science, 2001, **292** (5521).

H. Kao et al, A wide depth distribution of seismic tremors along the northern Cascadia margin, Nature, 2005, **436**.

K. Satake et al, Paleomagnetic correlation of late Holocene earthquakes among estuaries in Washington and Oregon, Nature, 1996, **378**, 246.

K. Wang et al, A revised dislocation model of interseismic deformation of the Cascadia subduction zone, Journal of Geophysical Research, 2003, **89**, 5763-5769.

W. E. Holt et al, Toward a continuous monitoring of the horizontal displacement gradient tensor field in southern California using cGPS observations from Plate Boundary Observatory (PBO), SRL, 2013, **84**, 455-467.

W. Szeliga et al, GPS constraints on 34 slow slip events within the Cascadia subduction zone, Journal of Geophysical Research, 2008, **113**, B04404.